

WAVE-CONVECTION COUPLING IN MULTICOMPONENT CONVECTION

Andrew STAMP and Ross W. GRIFFITHS

Research School of Earth Sciences
Australian National University
GPO Box 4, Canberra, ACT 2601, AUSTRALIA

ABSTRACT

Experiments with two-layer multicomponent convection in a rectangular cavity or annulus show that the convection spontaneously generates large-amplitude solitary waves which propagate along the interface. We use a layer of salt solution overlying a layer of sugar solution. The waves appear once the system evolves to a critical value of the density ratio $R_\rho = \alpha\Delta T/\beta\Delta S$. There are initially a number of waves. However, these interact with the convection until a single wave is left propagating back-and-forth along the length of the channel. Each wave causes horizontal variations in the buoyancy flux through the diffusive interface. The single wave organises tank-scale convective circulations in the layers, even in very long channels, and the wave-convection coupling leads to strong quasi-periodic reversals of the convective circulation. The wave continues to propagate indefinitely (while the layer properties are favourable). Thus energy exchange from the convection to the wave is important.

INTRODUCTION

The interaction of waves and convective flows is fundamental to many fluid flows. For example, travelling wave solutions are found for convective instability in binary fluids (Walden et al., 1985), and Langmuir circulation is thought to be driven by momentum transfer from surface waves. Another, more complex, example is the coupling of the El Nino - La Nina phenomenon in the equatorial Pacific with the Southern Oscillation in the atmospheric circulation of the Southern Hemisphere which involves interactions between the atmospheric convective circulations and waves in the equatorial ocean thermocline. Momentum, heat and water vapour transports across the air-sea interface are important.

The present investigation concentrates on the two-layer "diffusive" regime of multicomponent convection; specifically the salt/sugar system which involves two solutes with salt diffusing three times more rapidly than sugar. The diffusive interface separating two well mixed convecting layers has a stably stratified core with unstable boundary layers on either side. It is found that the convection may be strongly affected by the propagation of interfacial waves which modulate the interfacial buoyancy flux driving the convection. The consequent large-scale organisation of the convection, in turn, acts to maintain the wave-motion against dissipation. A quasi-periodic oscillation in the convective circulation persists.

DESCRIPTION OF EXPERIMENTS

Independent Parameters

In the case of two-dimensional flow in a rectangular tank, of length L and two layers of equal depth d the nondimensional parameters governing multicomponent convection are the tank aspect ratio L/d , the density-anomaly ratio $R_\rho = \Delta\rho_S/\Delta\rho_T$, the fractional density

difference $\Delta\rho/\rho_0$ across the interface, and parameters involving the molecular properties of the system (a Rayleigh number, a Prandtl number and the ratio of diffusivities κ_S/κ_T), where T and S refer to the properties having the greater (T) and the smaller (S) diffusivity. As this study is concerned with the propagation of waves along the double-diffusive interface it is most relevant to use the total density difference $\Delta\rho$ across the interface than the density difference $\Delta\rho_T$ or $\Delta\rho_S$ due to either component. Furthermore, we follow the convention of Griffiths and Ruddick (1980) and define R_ρ as

$$R_\rho = 1 + \frac{\Delta\rho}{\rho\alpha\Delta T} \quad (1)$$

where α is the expansion coefficient for T .

Experimental Apparatus and Procedures

In each experiment aqueous solutions of sodium chloride (T) and sucrose (S), dyed with blue and yellow water-soluble food dye, respectively, were mixed to desired densities. A single double-diffusive interface, separating two convecting layers of equal depth $d = 11.5$ cm, was set up by carefully floating the salt solution on top of the sugar solution through diffusers. Rectangular channels of length 15 cm (width 5 cm) and of length 15, 30, 60, 90, 135 and 180 cm (width 15 cm) were used. Other experiments are being carried out in an annular gap of width 5 cm and outer diameter 22.5 cm.

In order to calculate R_ρ and $\Delta\rho/\rho_0$ the layer properties were determined by measuring the density and conductivity of 5 ml samples taken from both layers at regular intervals. The Ruddick and Shirtcliffe (1979) polynomials relating density and conductivity to salt and sugar concentrations were used. Fluxes of salt and sugar through the density interface, and the consequent buoyancy flux, were also determined. The Rayleigh number of convection within each layer was of the order 10^9 - 10^{10} , depending on concentration differences and the time-dependent value of R_ρ . Hence convection was always turbulent.

The motions were made visible by a slide projector which illuminated the tank from the opposite side to that from which observations were made (the "back" of the tank). Two pieces of tracing paper were attached to the front of the tank so as to cover the upper and lower layers but not the double-diffusive interface. This produced a "shadowgraph" of the two layers and revealed the convective motions. A thin strip of tracing paper was attached to the back of the tank to act as a diffusing screen behind the double-diffusive interface. The stable core of the interface was easily distinguished from the upper and lower layers as a green region due to the mixing of the yellow and blue dyes. In other experiments, time-lapse photography was used to capture the motions of fine rheoscopic particles. Each visualization technique had to cover the length of the channel, up to 2 m.

The times at which the nose of the wave reached the tank

end walls were measured. Measurements of the thickness of the wave-head and -tail were also made at selected times during the cycle.

Three groups of experiments were completed in rectangular channels. In the first group all experiments were conducted in a tank of length $L = 15$ cm and the initial values of R_ρ and $\Delta\rho/\rho_0$ were varied so as to investigate wave-convection coupling over a wide range of layer properties and initial conditions. For the second group the 15 cm tank was used for each experiment and the initial conditions varied in such a way that R_ρ and $\Delta\rho/\rho_0$ evolved along the same path, thus allowing the starting criterion for wave-convection coupling to be determined. In the final group the effect of the tank aspect ratio was investigated by varying the tank length over the range $L = 15$ cm to 180 cm while having identical initial conditions in each experiment.

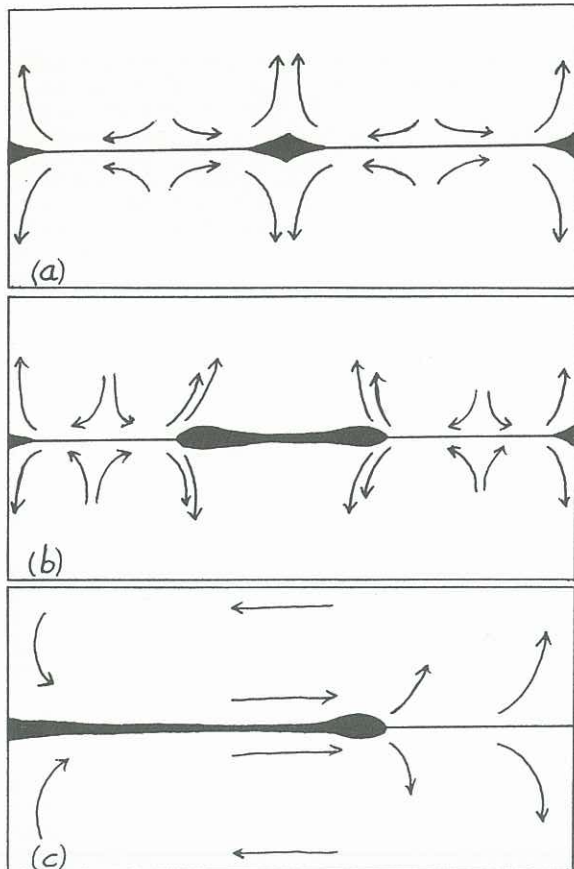


Fig.1. Diagrams of the system during the second stage, third and fourth stages of evolution described in the text. a) The interface is thickest and buoyancy flux greatest at the boundary between the two cells as a result of the sweeping action of the convective circulations. b) The formation of the two solitary waves from the gravitational collapse of the interface which occurs when the behaviour observed in the second stage becomes unstable. c) The interactions between the single solitary wave and convective circulations observed in the fourth stage of evolution. The situation shown is seen in each cycle soon after the large-scale circulation reverses and the wave begins to experience a wind in the same direction as its phase velocity.

RESULTS FOR RECTANGULAR CHANNELS

Observations

All of the experiments conducted in rectangular tanks evolved through four distinct stages. During the first stage the double-diffusive interface was very thin and horizontally uniform, apart from some small, very localized

thickening at points where plumes left the interface. The position of plumes was random and transient, with motions in the convecting layers consisting of regions of up- and down-welling separated by horizontal distances comparable to or smaller than the layer depth. These motions showed no coherence over larger distances, or over the whole length of the channel. After approximately 15 minutes (for $L = 15$ cm) the system evolved into a second stage which was characterised by the presence of two convective cells in each layer. As shown in Fig.1(a) the interface was thickest and buoyancy fluxes greatest at the boundary between the cells (where convection falls away from the interface) as a result of the sweeping action of the convective circulations.

The third stage commenced when the lump of interfacial fluid supported by the convective circulation became gravitationally unstable and collapsed, forming two solitary waves moving in opposite directions as shown in Fig.1(b). This occurred typically 30 minutes after the start of the experiment. Once the two waves formed they propagated back-and-forth across the tank, interacting with each other. During this stage the convection in the mixed layers showed no sign of a structure on the scale of the tank length.

In the final stage a single solitary wave formed out of the two-wave regime. This transition occurred when both waves happened to be near the same end of the tank, where together they reduced the buoyancy flux by thickening the interface. At the other end of the channel the interface was thin and transferred a large buoyancy flux. The horizontal gradients thus established over the length of the channel in each convecting layer forced a circulation along the channel. This tank-scale cell assisted the single wave propagating across the tank. The horizontal variation in buoyancy flux was due to the fact that the thinner interface away from the wave results in large S and T gradients and hence large diffusive fluxes. Once a single wave was set up it propagated back-and-forth across the tank interacting with the convection in the manner shown in Fig.1(c).

The waves may be considered to consist of two portions: a propagating solitary wave head followed by a tail of mixed fluid. The interfacial fluid in the tail is acted upon by gravity and by a stress exerted by the surrounding convective motion. During a first portion of the wave propagation from one end to the other the wave propagates into a head-wind, which slows its motion relative to the tank and prolongs the period during which the interface is thick at the end away from which the wave is moving. The circulation then reverses and the tail is swept along with the wave head. Although the head is defining the position of the wave, it is the tail that is largely responsible for the length-scale of horizontal variations in the interface thickness and buoyancy flux.

Starting Criterion for Wave-Convection Coupling

Figs.2 and 3 show the evolution of R_ρ and $\Delta\rho/\rho_0$ for each experiment in the first two groups of runs described earlier. The positions corresponding to the start of tank-scale circulation due to wave-convection coupling are labelled. In each case a value of R_ρ can be assigned to the time at which the coherent horizontal motion begins. Since the values are similar, we conclude that R_ρ must exceed a critical value $R_\rho^c \approx 1.14$ for wave-convection coupling to occur.

A physical argument supporting the concept of a critical density ratio for onset of effective coupling can be made by noting that the phase speed for deep-water solitary waves $c \propto a\sqrt{\Delta\rho}$, where a is the wave amplitude (Stamp and Jacka, 1992; Stamp and Griffiths, this volume), and by assuming that for wave-convection coupling the wave speed and horizontal convective velocities must be comparable. At the start of an experiment the buoyancy fluxes and resulting convective velocities are very large because the double-diffusive interface is very thin. Consequently, wave amplitudes and speeds are too small to couple effectively with the convective velocities. As the system runs-down the interface thickens, thus supporting larger, and faster, waves which can cause horizontal variations in the buoyancy flux large enough to organise convective circulations. Also, the buoyancy flux and convective

velocities decrease. At some point the wave speeds are large enough and the convective velocities small enough for coupling. Since the wave amplitude and convective velocities are controlled by the interface thickness, and this is a strong function of R_ρ , it is expected that a critical value of R_ρ must be exceeded before coupling can occur.

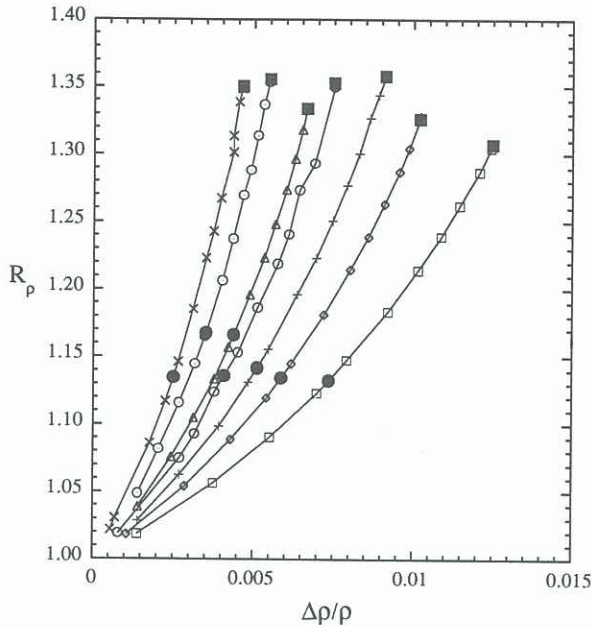


Fig.2. The density anomaly ratio R_ρ plotted against density difference $\Delta\rho/\rho_0$ for some of the first set of experiments (● – onset of tank-scale circulation coupled to a single wave; ■ – wave and circulation die out when the interface becomes too thick).

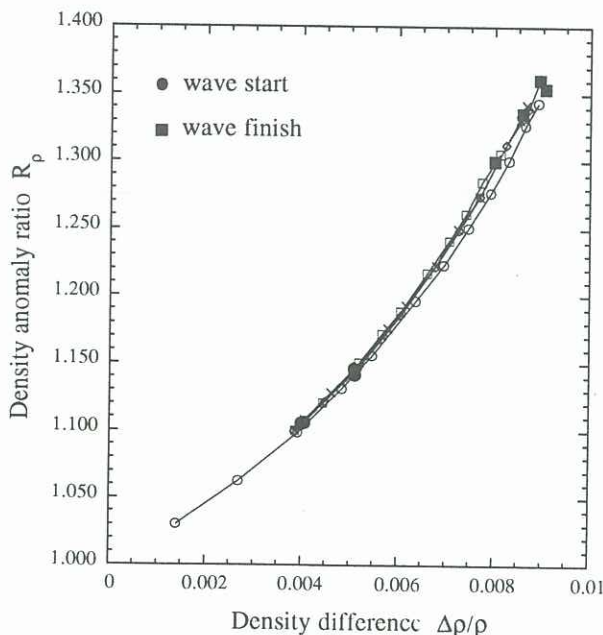


Fig.3. The density anomaly ratio R_ρ plotted against density difference $\Delta\rho/\rho_0$ for the second set of experiments in which the system was established with different initial conditions but evolved along the same path.

The above argument can be made more quantitative by writing the wave speed c and horizontal convective velocity u in the forms

$$c \sim \left(\frac{g\Delta\rho}{\rho_0}\right)^{1/2} a; \quad u \sim (q_B L)^{1/3}, \quad (2)$$

where a is the wave amplitude and q_B is the interfacial buoyancy flux. Requiring $c = u$ leads to

$$c \sim (q_B L)^{1/3}$$

$$a \sim \left(\frac{g\Delta\rho}{\rho_0}\right)^{-1/2} (q_B L)^{1/3} \quad (3)$$

$$T \sim q_B^{-1/3} L^{2/3},$$

where T is the oscillation period.

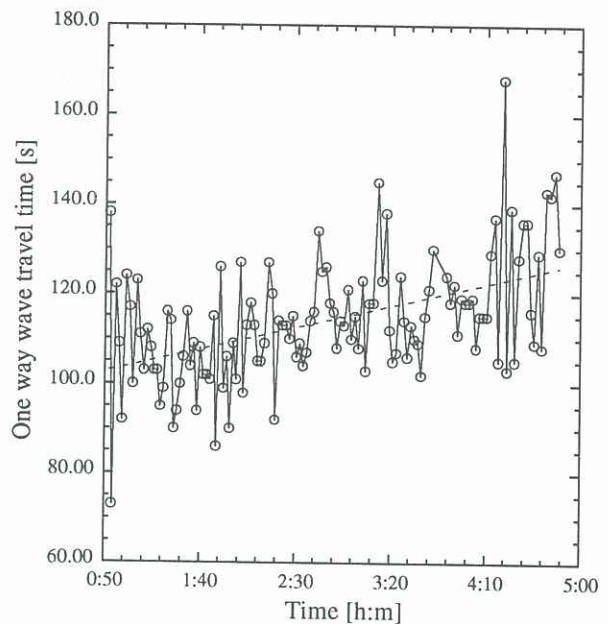


Fig.4. A plot of the time taken for the wave to travel across the tank ($L = 15$ cm) against the time since the start of one experiment.

Run-Down Effects on Wave-Convection Coupling

Fig.4 shows the time taken for the wave to travel the tank length plotted against time for one experiment. Variations occur on two time scales: a short time scale associated with complex wave-convection dynamics under the instantaneous conditions, and a long time scale associated with the run-down.

The qualitative behaviour of the wave-convection coupling remained unchanged during run-down. However, there are several quantitative aspects which change slowly with time: the average thickness of the double-diffusive interface increases, the buoyancy fluxes and convective velocities decrease and the wave speed decreases. Fig.5 shows a contour plot of the one way travel time as a function of R_ρ and $\Delta\rho/\rho_0$. The increase in travel time with increasing R_ρ is a result of the decrease in convective velocities, whereas the decrease in travel time with increasing $\Delta\rho/\rho_0$ is due to the $c \propto \sqrt{\Delta\rho}$ relationship.

Effects of Channel Aspect Ratios

The same qualitative behaviour was observed in both short (15 cm) and long (180 cm) channels. In the latter the convection in each layer at $R_\rho > R_\rho^c$ formed a long, flat circulation cell of aspect ratio 0.064, whose direction

reversed every 10 to 20 minutes. A longer channel length leads to larger horizontal convective velocities (2) once the convection becomes organised over the tank length. This, in turn, demands a greater interfacial wave speed (3) for coupling. However, these larger wave speeds and the strong coupling cannot occur until the interface is thicker than it is at onset of coupling in shorter channels. Hence the critical value of R_p is larger.

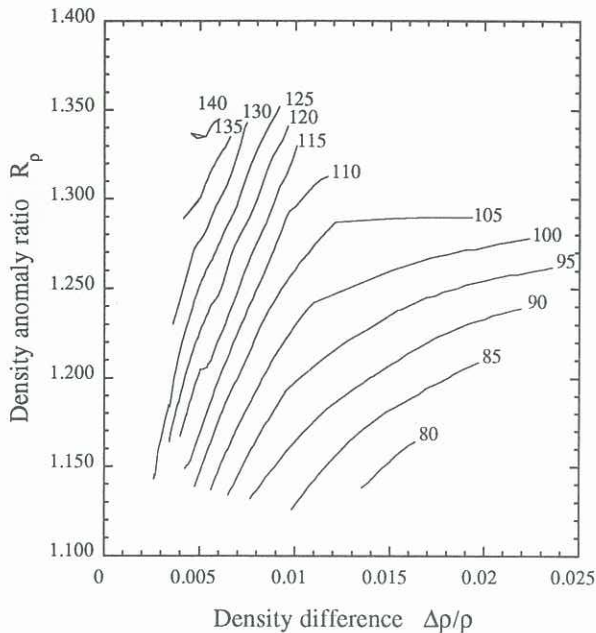


Fig.5. A contour plot of the time taken for waves to travel across the tank ($L = 15$ cm) as a function of convecting layer properties. Numbers on contours are the one-way travel time in seconds.

ANNULUS EXPERIMENTS

At present only preliminary observations of wave-convection coupling in an annular gap have been obtained. While it remains unclear as to how the waves are formed in this geometry wave-convection coupling is still observed. Typically four waves, each with two associated convection cells in each layer, are observed initially. As was the case during much of each wave cycle in rectangular tanks, the annulus waves propagate into a head wind. The number of waves evolves with time, decreasing to three, then two and finally one. This elimination process occurs when a faster moving wave overtakes a slower wave. When there is a single wave, the tail of mixed fluid and two convection cells in each layer extend half way around the annulus. The wave and convection cells propagate around the annulus in the same direction until the coupling is finally destroyed by dissipation due to viscous effects at the walls.

CONCLUSIONS

Coupling of solitary interfacial gravity waves with turbulent high-Rayleigh number convection can occur in two-layer systems and leads to organisation of the convective motions over large horizontal length scales. The coherent motions propagate as a travelling wave linked to the interfacial gravity wave and, in a channel, give rise to reversals of the circulation observed at a fixed point in space. In a narrow channel of finite length the scale of coherence is the full length of the channel. In this case a standing wave flow pattern is established and we observe quasi-periodic flow reversals throughout the channel. Coupling is effective at organising the convective circulation when the wave speeds are comparable to the horizontal convection velocities driven by the buoyancy

flux through the density interface. Hence coupling occurs when the mean interface thickness is large enough to support nonlinear waves of sufficient amplitude and speed to match the convective velocities, but not so thick as to greatly reduce the buoyancy flux and convective velocities. Further work is being carried out on the annular geometry, where end-wall reflections and their effects on phase relationships between waves and the induced circulation are absent.

The wave-like behaviour observed in the two-layer double-diffusive system is maintained by a transfer of energy from the buoyancy flux to the organised convective circulation and, in turn, to the interfacial wave. The process can be viewed as a negative feedback mechanism: when the wave crest is at one end of a finite channel the interface there is thicker, the buoyancy flux is reduced (or switched off), and the circulation in each layer is forced to reverse. This very striking phenomenon bears some similarity to the coupling of the tropical Pacific thermocline to the overlying Trade winds, which leads to the El Nino-Southern Oscillation. Considering the equatorial channel, a longitudinal gradient of interfacial buoyancy flux again helps to organise convective circulation over the width of the Pacific, and momentum transfer from this circulation to the upper ocean leads to internal waves and a set-up of the tropical thermocline. There is, however, an important difference between the two systems. Larger sea-to-air heat and moisture fluxes in the western Pacific tend to strengthen the westerly winds, leading to a larger warm pool in the western Pacific and larger fluxes. This is a positive reinforcement that tends to maintain the 'normal' state of the system. Similarly, a reduction of the western Pacific thermal anomaly (a reduced longitudinal gradient of surface fluxes) can weaken the Trades which, in turn, leads to a further decrease in the east-west sea-surface temperature difference. Thus the Equatorial Pacific appears to be dominated by a forcing that tends to maintain the existing circulation, whereas in the double-diffusive oscillation studied here the buoyancy fluxes oppose the existing circulation throughout much of each cycle.

REFERENCES

- GRIFFITHS, R W and RUDDICK, B R (1980) Accurate fluxes across a salt-sugar finger interface deduced from direct density measurements. *J Fluid Mech.* **99**, 85.
- RUDDICK, B R and SHIRTCLIFFE, T G L (1979) Data for double diffusers: Physical properties of aqueous salt-sugar solutions. *Deep-Sea Res.* **26A**, 775.
- STAMP, A and GRIFFITHS, R W (1992) Large-amplitude mode 2 deep-water internal solitary waves. This volume.
- STAMP, A and JACKA, M (1992) Large-amplitude mode 2 deep-water internal solitary waves. *J Fluid Mech.* submitted.
- TURNER, J S (1985) Multicomponent convection. *Ann Rev Fluid Mech.* **17**, 11.
- WALDEN, R W, KOLODNER, P, PASSNER, A and SURKO, C M (1985) Travelling waves and chaos in convection in binary fluid mixtures. *Phys Rev Lett.* **55**, 496.